Normal Form approaches and resonance analysis of LHC models

Yannis Papaphilippou and Frank Schmidt

CERN,
CH-1211 Geneva 23
Switzerland

Abstract. In order to understand the dynamic aperture limitations in LHC optics versions 4 and 5 at injection energy (450 GeV), a thorough resonance analysis is performed through Lie perturbation methods and Normal Form construction. In this respect, a simple numerical tool has been developed, the Graphical Representation of Resonances (GRR), allowing the evaluation and graphical representation of the resonance strengths and detuning, up to a desired order. The resonance analysis performed by means of GRR enabled us to understand the effect of the large errors in some special quadrupoles of LHC optics version 5. We were also able to identify and minimise the resonance which was correlated with the drop of the dynamic aperture, following the introduction of a large skew octupole bias in the LHC optics version 5, using the "target" error table. As shown by subsequent tracking studies, the proposed correction procedures led to a considerable improvement of the dynamic aperture of the studied LHC models.

INTRODUCTION

A crucial point in the design of hadron colliders is the long term beam stability determined by the dynamic aperture (DA). The straightforward procedure to calculate the DA of a given accelerator model is performed through element by element tracking of particles. Considering the fact that the usual injection time for accelerators like the LHC corresponds to 10^7 particle turns, tracking simulations are limited by the lack of available computer power for following the full particle orbits. A more serious problem comes from the fact that tracking cannot provide any understanding regarding the resonance structure in the phase space of the system. What seems to be of high interest is to recover the reasons triggering these resonances thereby limiting the DA.

The necessary insight regarding the system's non-linear dynamics can be given by applying the methods of high order perturbation theory [1–3]. These approaches can be conducted by using an explicit form of the system's Poincaré map. This map is usually computed through a Taylor expansion around the 1-periodic orbit

of the accelerator beam, with the assistance of Lie algebraic tools. In general, the map is written in variables which are not close to the invariants of motion. The construction of Normal Forms consists in transforming the original variables of the map to a new set of variables, which are close to the invariants of motion, in order for the resulting map to have a simpler form. The generating function, through which this symplectic transformation is performed, is computed by means of a perturbative scheme using as parameter the distance to the origin. This function contains the information regarding the distortion of the phase space due to non-linearities and the influence of resonances on the dynamics of the system.

On the other hand, what could be of great interest is an indication about the resonance strengths for specific initial conditions, especially close to the parts of the phase space where the beam is lost. This is a key point for coping with the non-linear dynamics of an accelerator, taking into account that particular multipolar magnet errors have a specific contribution to particular resonance strengths. Thus, the resonance strengths establish a sort of quality factor [6], which can determine whether the specifications proposed for the design of an accelerator lattice are optimal with respect to the phase space regularity of the model. Through a resonance analysis of this kind, one can associate the physical characteristics of the accelerator to the DA of the model, find the limits and provide the necessary cures, ensuring the long-term stability of the beam. In this respect, we developed a simple numerical tool, the Graphical Representation of Resonances (GRR), which uses as input the output of standard Lie algebraic numerical codes [4] and allows the evaluation and graphical representation of the resonance strengths and detuning, up to a given order (see also [5,6]).

In this article, we present the impact of the use of GRR in the ongoing studies for understanding the dynamics of the LHC optics versions 4 and 5. The article is organised as follows: in Sect. I, we outline the basic ideas regarding Normal Form analysis and the GRR tool. In the next section, we present examples of the application of this resonance analysis in order to understand the dynamics of LHC models. In the last section, the principal results are summarised together with some objectives for future studies.

I GRAPHICAL REPRESENTATION OF RESONANCES

A Resonance strength

By neglecting the weak coupling between the vertical and horizontal motion and the longitudinal one, the system is restricted to the 4D phase space. In order to construct the Normal Form $\mathcal{U}$ of a Poincaré map $\mathcal{M}$ representing the successive intersections of a kicked accelerator beam at a fixed position of the path variable

s, one performs a symplectic transformation expressed by the functional equation

$$\mathcal{U} = \Phi^{-1} \circ \mathcal{M} \circ \Phi \ ,$$

which transforms the variables of the original map $\mathbf{z} = (z_x, z_x^*, z_y, z_y^*)$ to a new set $\boldsymbol{\zeta} = (\zeta_x, \zeta_x^*, \zeta_y, \zeta_y^*)$, where the $(*)$ denotes complex conjugate variables. The original variables are usually the complexified version of the Courant-Snyder coordinates

$$z_{x,y} = \sqrt{2\ J_{x,y}}\ e^{-i(\varphi_{x,y}+\varphi_{x0,y0})} \ , \tag{1}$$

where $J_{x,y}$ and $\varphi_{x,y}$ are the action-angle variables of the integrable problem, in the linear case. The actions are a function of the horizontal and vertical emittance

$$\epsilon_x = 2\ J_x = n_\sigma(\epsilon_n/\gamma)^{1/2}\cos\phi \quad \text{and} \quad \epsilon_y = 2\ J_y = n_\sigma(\epsilon_n\gamma)^{1/2}\sin\phi \ , \tag{2}$$

where the normalisation factor n_σ determines the amplitude of the particle in terms of the rms beam size σ, ϵ_n is the normalised emittance, γ the energy factor and ϕ is the amplitude ratio ($\tan\phi = \epsilon_y/\epsilon_x$).

On the other hand, the new variables are expressed

$$\zeta_{x,y} = \sqrt{2\ I_{x,y}}\ e^{-i(\psi_{x,y}+\psi_{x0,y0})} \ , \tag{3}$$

i.e. as a function of the non-liner invariants of motion $I_{x,y}$ and their conjugate phases $\psi_{x,y}$.

The transformation Φ, as well as the maps, may be represented using the Lie formalism, e.g.:

$$\Phi = e^{:F:} \ , \tag{4}$$

which denotes a series of Poisson brackets operations. In general, the generating function F is represented by a sum of homogeneous polynomials of the new variables. By taking the inverse transformation Φ^{-1}, the generating function F can be expressed as a function of the old variables

$$F = \sum_{jklm} f_{jklm}\ {z_x}^j\ {z_x^*}^k\ {z_y}^l\ {z_y^*}^m \ \text{ with } \ f_{jklm} \in \mathbb{C} \ \text{ and } \ j,k,l,m \in \mathbb{N} \ . \tag{5}$$

Inserting the expressions of the $\mathbf{z}$ variables in the series (5), one obtains:

$$F = \sum_{jklm} f_{jklm}\ (\epsilon_x)^{\frac{j+k}{2}}\ (\epsilon_y)^{\frac{l+m}{2}} e^{-i\varphi_{jklm}} \ , \tag{6}$$

where the phase term variable is $\varphi_{jklm} = (j-k)(\varphi_x + \varphi_{x0}) + (l-m)(\varphi_y + \varphi_{y0})$. The expression (6) is usually computed order by order by means of Lie algebraic numerical tools, as the DaLie code [4], which is used in the present study.

The infinite series (6) is not convergent by construction. Furthermore, the number of terms grows very sharply with the order $n = j+k+l+m$ [1–3]. In practice,

one takes a truncated expression of the series (6), and in our case, we usually found sufficient to carry out the calculation of the perturbing series up to 12th order which corresponds to an 11th order map.

The expression of the phase φ_{jklm} shows that each term of the series (6) corresponds to a resonance condition of the form

$$(j-k)\nu_x + (l-m)\nu_y + c = 0 \;\text{ with }\; c \in \mathbb{Z}\ ,$$

with ν_x and ν_y representing the frequencies of motion. These resonances are related with the non-linear dynamical behaviour of the system. The norm of the coefficients $|f_{jklm}|$ provides an indication about the strength of the corresponding resonances, these last being associated with the multi-polar magnetic field errors. In fact, multipole errors of a certain order n_m will have a contribution to the coefficients f_{jklm} of order $n \geq n_m$. Hence, one could infer that the importance of a specific resonance regarding the dynamics of the system can be revealed by the norm of the corresponding coefficients. However, the series terms associated with the same resonance $(a,b) = (j-k, l-m)$ of order n will also appear in higher orders $n+n'$, with n' a non-zero pair number. Thus, a more precise estimation of the resonance strength in a given position of the phase space can be efficiently computed only by including the contribution of these higher order terms. To do this, one may fix the phase at an arbitrary value, e.g. $\varphi_{jklm} = 0$, without loss of generality. The strength of a specific resonance (a,b) is given by the norm of

$$F_{(a,b)} = \sum_{\substack{jklm \\ j+k+l+m \leq n \\ j-k=a\ ,\ l-m=b}} f_{jklm}\ (\epsilon_x)^{\frac{j+k}{2}}\ \ (\epsilon_y)^{\frac{l+m}{2}}\ , \tag{7}$$

where the contribution of all terms up to an order n is taken into account.

B Tune shift

In the same way, one can also compute the tune shift due to the non-linearities of the system. In fact, in the non-resonant case, the variables $\zeta'_{x,y}$ after one conjugation of the map $\mathcal{U}$ are:

$$\zeta'_{x,y} = e^{-i\Omega_{x,y}(\rho_x,\rho_y)}\zeta_{x,y}\ , \tag{8}$$

where $\Omega_{x,y}$ are the non-linear frequencies associated with the horizontal and vertical motion and $\rho_{x,y} = 2I_{x,y} = \zeta_{x,y}\zeta^*_{x,y}$ are the generalisation of the vertical and horizontal emittance in the non-linear case. Taking into account that the tunes are

$$\Omega_{x,y} = \frac{\partial\, \overline{H}}{\partial \rho_{x,y}} \tag{9}$$

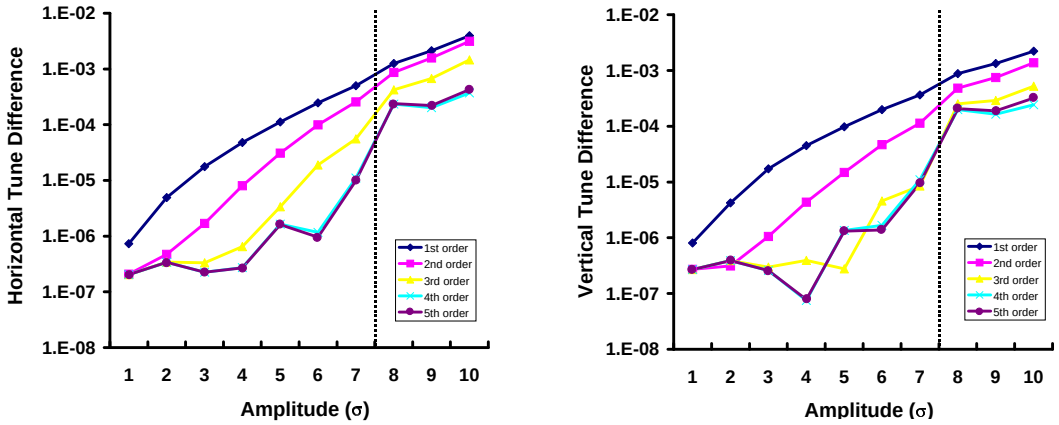

FIGURE 1. *Difference between the tune values calculated with two methods, for a specific realisation of the magnet errors (seed 25) of LHC optics version 5 "nominal" table, for $\phi = 15°$ and for different particle amplitudes.*

where $\overline{H}$ is the new Hamiltonian associated with the map, the non-linear tunes can be written as a series of homogeneous polynomials

$$\Omega_{x,y}(\rho_x, \rho_y) = \sum_{\substack{jklm \\ j+k+l+m \leq [(n-1)/2] \\ j-k=0\ ,\ l-m=0}} \omega_{jklm} \left(\rho_x\right)^{\frac{j+k}{2}} \left(\rho_y\right)^{\frac{l+m}{2}} \quad , \tag{10}$$

where the (j, k, l, m) are such that the phase dependence vanishes, leaving only the amplitude dependent terms in the polynomial. In order to evaluate the series (10), the knowledge of the non-linear invariants $\rho_{x,y} = 2I_{x,y}$ is necessary. These last can be computed through the inverse transformation $\Phi^{-1}(\mathbf{z})$. Hence, the non-linear invariant can be expressed as a function of the linear ones $\epsilon_{x,y}$ and the non-linear tunes can be calculated by the series (10) written in these latter variables. Note also that the maximum detuning order is now the integer part of the expression $(n-1)/2$, e.g. the terms of an 11th order map will contribute up to a detuning order of 5.

The precision of the calculation using the Normal Form machinery can be checked by comparing the tunes computed through the series expansion (10) with the values provided by a direct application of a Laskar type frequency analysis [7] (we use the the SUSSIX code [8]) of tracking data generated by SIXTRACK [9] for several particle orbits, in the case of the "nominal" error table of LHC optics version 5. We generated 10 particle orbits, the amplitude of which varies from $n_s = 1\sigma$ to 10σ and the amplitude ratio is kept fixed $\phi = 15°$. In Fig.1, we present graphically the difference between the horizontal (left) and vertical (right) tune given by the two computation methods for a specific realisation of the magnet errors ("seed" number 25) . The different graphs correspond to different orders in the calculation of the tune (from 1st to 5th order) and the horizontal axis corresponds to different amplitudes measured in σ. The vertical axis represents the tune difference in logarithmic

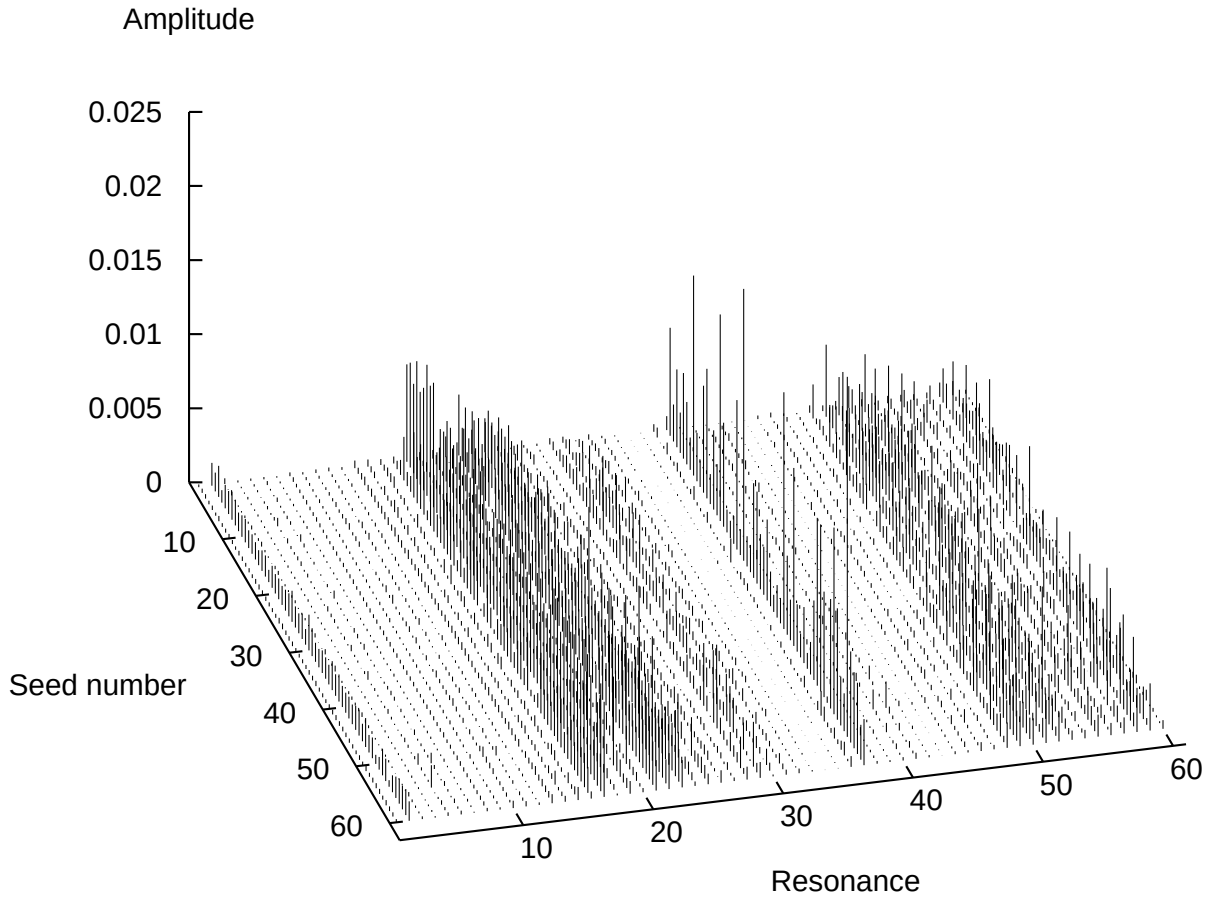

FIGURE 2. *Norm of the 7th order resonance coefficients f_{jklm} of the generating function (6), for 60 seeds of LHC optics versions 5 using the "nominal" error table.*

scale and the vertical doted line denotes the barrier after which the particles begin to be chaotic. It is apparent that, at least up to the point where the particles are stable and after adding the 4th order contribution, the two approaches converge to the same value, with a precision of 10^{-5}. Let us just remark that this result is only valid for a regular orbit evolving on a KAM torus. For a chaotic orbit, the calculation becomes meaningless as the tune is not constant.

II APPLICATION TO THE LHC

A Limitations in the dynamic apperture of LHC optics versions 4 and 5

A global picture of the resonance strengths given by the generating function F is represented graphically in the 3D plot of Fig. 2. This graph represents the norm

of the 7th order resonance coefficients f_{jklm} with $n = 7$, for LHC optics version 5, using the "nominal" error table and for 60 seeds. Each number on the horizontal axis corresponds to a different 7th order resonance (60 in total - see Table 1). The first 7 series of spikes represent the amplitudes of the normal resonances and the next 23 the normal sub-resonances. The remaining 30 correspond to the 7th order skew resonances and sub-resonances.

The importance of the (7,0) resonance for predominantly horizontal motion was reported in previous studies [10,11]. Nevertheless, this is not at all visible in this picture, i.e. the first series of spikes is quite small as compared with certain sub-resonances and skew resonances, in the middle of the graph. This is indeed due to the fact that the subresonance strengths mask the importance of the (7,0) resonance. On the other hand, the higher order series terms contributing to a specific resonance are not included in the coefficients f_{jklm}.

Through Eq.(7), we were able to evaluate the strength $\left|F_{(a,b)}\right|$ of the 7th order resonances up to 12th order, for an amplitude ratio of 15° at 8σ, which is close to the minimum DA of this LHC model. A graphical representation of these resonances (14 in total) is given in Fig. 3. The depicted points correspond to the average value of the resonance driving terms over the 60 random realisations of the magnet

TABLE 1. Correspondence of numbers labelling the horizontal axis of Fig. 2 with the 7th order resonances

	resonances		sub-resonances					
	7th order		5th order		3th order		1st order	
	(j,k,l,m)	N_o	(j,k,l,m)	N_o	(j,k,l,m)	N_o	(j,k,l,m)	N_o
Normal	(7,0,0,0)	1	(6,1,0,0)	8	(5,2,0,0)	18	(4,3,0,0)	27
	(5,0,2,0)	2	(5,0,1,1)	9	(4,1,1,1)	19	(3,2,1,1)	28
	(3,0,4,0)	3	(4,1,2,0)	10	(3,0,2,2)	20	(2,1,2,2)	29
	(1,0,6,0)	4	(3,0,3,1)	11	(3,2,2,0)	21	(1,0,3,3)	30
	(5,0,0,2)	5	(2,1,4,0)	12	(2,1,3,1)	22		
	(3,0,0,4)	6	(1,0,5,1)	13	(1,0,4,2)	23		
	(1,0,0,6)	7	(4,1,0,2)	14	(3,2,0,2)	24		
			(3,0,1,3)	15	(2,1,1,3)	25		
			(2,1,0,4)	16	(1,0,2,4)	26		
			(1,0,1,5)	17				
Skew	(6,0,1,0)	31	(5,1,1,0)	38	(4,2,1,0)	48	(3,3,1,0)	57
	(4,0,3,0)	32	(4,0,2,1)	39	(3,1,2,1)	49	(2,2,2,1)	58
	(2,0,5,0)	33	(3,1,3,0)	40	(2,0,3,2)	50	(1,1,3,2)	59
	(0,0,7,0)	34	(2,0,4,1)	41	(2,2,3,0)	51	(0,0,4,3)	60
	(6,0,0,1)	35	(1,1,5,0)	42	(1,1,4,1)	52		
	(4,0,0,3)	36	(0,0,6,1)	43	(0,0,5,2)	53		
	(2,0,0,5)	37	(5,1,0,1)	44	(4,2,0,1)	54		
			(4,0,1,2)	45	(3,1,1,2)	55		
			(3,1,0,3)	46	(2,0,2,3)	56		
			(2,0,1,4)	47				

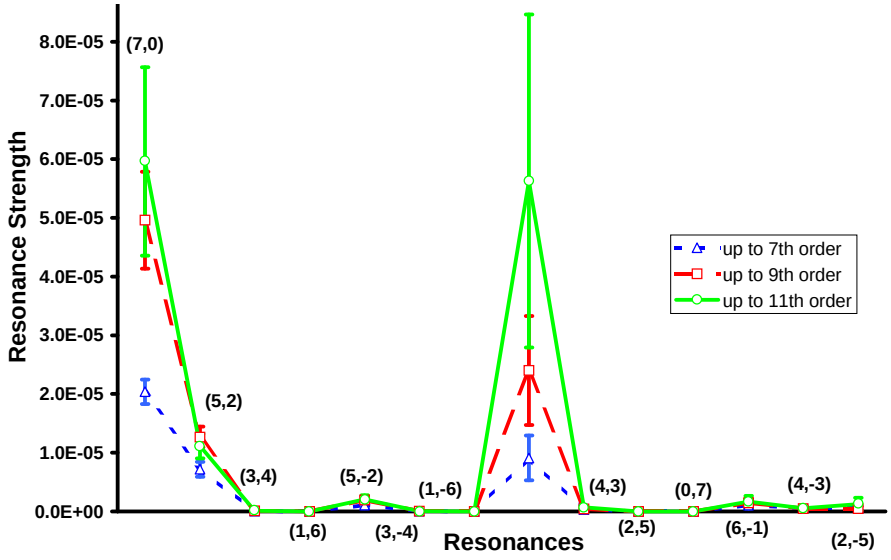

FIGURE 3. *Average value and standard deviation of the 7th order resonance strength at* 8σ *and* $\phi = 15°$ *for LHC optics version 5 "nominal" error table, over 60 seeds. The three different graphs represent resonance driving terms computed up to 3 different orders.*

errors and the error bars are equal to one standard deviation. The three different lines represent resonance strengths the computation of which is conducted up to 3 different orders (7th, 9th and 11th). It is now clear that the (7,0) resonance has a quite big influence in the dynamics of the system. Moreover, the contribution of the higher orders to this resonance are quite important, a fact which could have not been revealed by simply checking the coefficients of the function F (Eq. 6). On the other hand, this graph also shows that the strength of the (6,1) resonance is quite big. A further analysis of the detuning of the system reveals that at this part of the phase space, the particle tunes are close to this resonance.

By using GRR, we were able to understand the reason for this strong excitation of the (7,0) resonance, limiting the DA of LHC optics version 5 with respect to version 4, at least for motion close to the horizontal plane. It was found that the large multi-pole errors corresponding to some special type of quadrupoles ("warm" quadrupoles) on the two high-beta insertions (I.P.3 and I.P.7) of the LHC optics version 5 were in the heart of the problem [13]. In Fig. 4, we present the average (over 60 seeds) absolute value of the relative difference, that is the difference of the resonance strength weighted by the biggest one among the two, between the 12 most prominent resonances of LHC optics version 4 and 5. There is a 50% difference between the amplitudes of the (7,0) resonance in the two lattices. By switching off the errors in the "warm" quadrupoles, the two lattices become approximately identical. This effect is indeed due to the strong kick produced by the interplay of the important beta function values in these areas of the machine (of the order of 350 m in I.P. 3 and 600 m in I.P.7 [14]) with the strong multi-pole errors of the

TABLE 2. The effect of the multipole errors of warm quadrupoles on the dynamic aperture for different LHC optics versions 4 and 5 machines. The average and minimum DA over 60 seeds is shown, for $\phi = 15°$ and $45°$.

Phase	Type	DA (σ)	LHC Version		
			4	5	
				Nominal	Target
15°	Warm Quads switched ON	Average	10.0	9.1	10.4
		Minimum	8.5	7.4	8.6
	Warm Quads switched OFF	Average	10.7	11.6	12.4
		Minimum	9.6	10.3	11.3
45°	Warm Quads switched ON	Average	11.1	11.3	12.8
		Minimum	9.5	9.2	11.4
	Warm Quads switched OFF	Average	11.4	12.4	13.8
		Minimum	10.1	10.7	12.3

"warm" quadrupoles (especially the b_3 and b_7).

This resonance analysis study guided us in the correction of the LHC optics version 5 with an important average improvement of the DA. The results of the 6-dimensional tracking studies with SIXTRACK [9] are reported in Table 2. We give the minimum and average value of the DA for several cases of LHC optics version 4 and 5, with and without the errors in the "warm" quadrupoles. The "target" error table is the one proposed in order for the LHC to reach the target DA of 12σ so as to have a safety factor of 2 [11], considering the fact that the collimators will be positioned at 6σ. The tracking is conducted for two directions of the phase space (amplitude ratios of 15° and 45°) which, in our case, correspond roughly to the minimum and average values of the DA, over all phases [15]. For all cases and for both phase values, the average gain of the D.A. is of the order of 2σ. Especially for the "target" error table, we are able to reach the target DA of 12σ.

B Correction of the effect of the octupole error bias on the LHC dipoles

A similar resonance analysis was followed in order to understand the drop of the DA in LHC optics version 5, using the "target" error table, after the inclusion of a large bias of the systematic per arc octupoles in the main dipoles of the model [16]. Indeed, the inclusion of these new realistic values for the octupole errors deteriorated the DA of the "target" table (see Table 3, "strong b_4", "strong a_4" and "strong b_4, a_4" cases).

The experience from LHC optics version 4 [10] has shown that the bias can be usually cancelled by erect and skew octupole spool pieces in half of the machine,

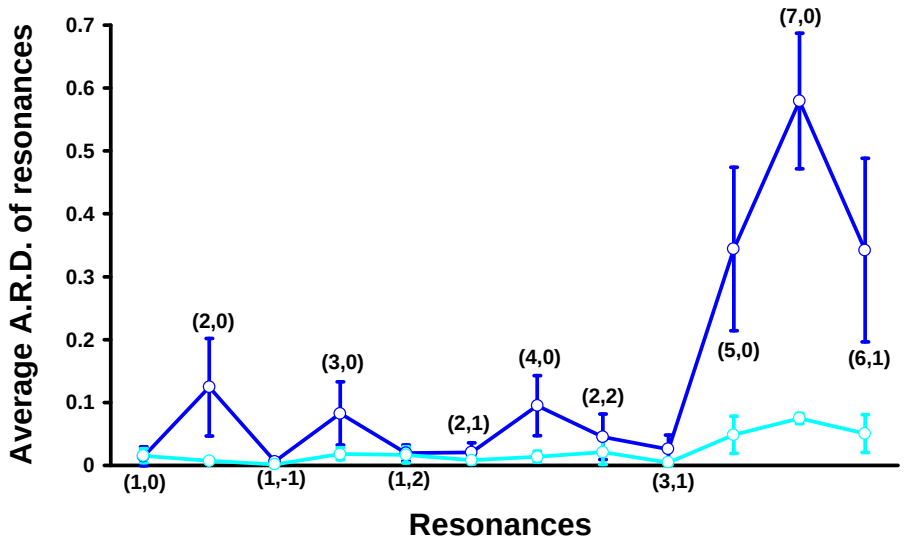

FIGURE 4. *Average absolute value of the resonance strengths relative difference at* 8σ *and* $15°$ *between LHC optics version 4 and 5 with and without the errors on the "warm" quadrupoles.*

TABLE 3. The effect of realistic erect and skew octupolar errors and their corrections on the dynamic aperture of LHC optics version 5 at injection. The average and minimum DA over 60 seeds is shown, for $\phi = 15°$ and $45°$.

Errors and Correctors	Phase [°]			
	15		45	
	Dynamic Aperture [σ]			
	Minimum	Average	Minimum	Average
Target error table	11.3	12.4	12.3	13.8
Strong b_4	9.6	12.2	10.8	13.4
$+b_4$ spool piece (SP)	11.8	12.6	12.0	13.7
Strong a_4	10.4	12.1	10.0	12.9
$+a_4$ SP	10.2	12.1	9.5	12.5
+ optimised a_4 SP	11.3	12.5	11.7	13.8
Strong b_4, a_4	10.1	12.0	10.0	12.6
$+b_4$ SP, a_4 SP	9.7	12.0	9.5	12.5
$+b_4$ SP, optimised a_4 SP	11.2	12.6	11.8	13.6

each located at one end of the dipoles and powered in series (having one spool piece type in the outer channel corresponding to the 1st, 5th, 6th and 7th octant and one in the inner channel corresponding to the remaining octants). The correction of the bias of the erect octupole component with erect octupole spool pieces in half of the machine fully restored the DA of the "target" error table (see Table 3, "$+b_4$ spool piece" case). Nevertheless, it was not sufficient to suppress the bias of the

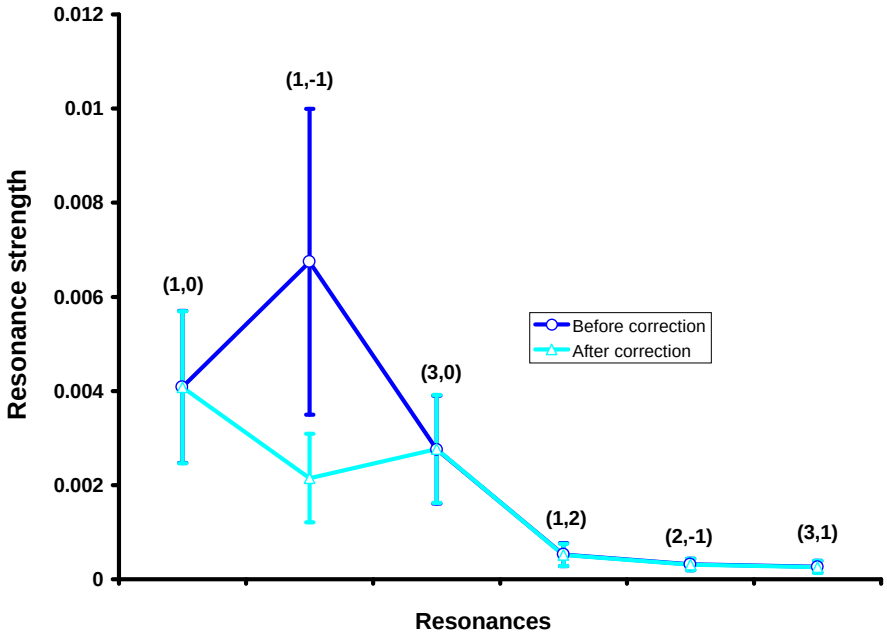

FIGURE 5. *Strength of resonances for LHC optics version 5 due to skew octupole errors before and after correction.*

skew octupole component following the same procedure (see Table 3, "+$a4$ SP" and "+b_4 SP, a_4 SP" cases).

A resonance analysis with GRR has revealed that the skew octupoles mainly excite the (1, –1) resonance. In order to cancel the effect of the skew octupoles, a minimisation procedure was followed, by producing maps parameterised by the strength of the skew octupole spool pieces. The minimisation of the first order coefficients f_{1012}, f_{2101} of the (1, –1) resonance with skew octupole spool pieces positioned in the outer channel of the LHC lattice and powered in series was very beneficial. This can be easily seen in Fig. 5 where we present the strength difference of some important resonances between the "target" error table and the tables with the large skew octupole bias before and after the correction. The resonances in this graph are evaluated at an amplitude of 8σ and for amplitude ratio of 15°. All points represent the average values over 60 seeds and the error bars correspond to the standard deviation. The effect of the correction of the (1, –1) resonance is indeed very visible. The resonance strength are considerably reduced after the correction with the skew octupole spool pieces. In particular, the (1, –1) resonance strength decreases by a factor of three so that there is approximately no difference left with the one of the "target" error table. This improvement was verified by the tracking studies, where the D.A. is fully restored after the correction with respect to the one of the initial "target" error table (Table 3, "optimised a_4 SP" and "+b_4 SP, optimised a_4 SP" cases).

III CONCLUSIONS

We followed a resonance analysis procedure in order to understand the reasons which limit the DA of LHC optics version 4 and 5. For this, we used the standard Normal Form approaches of Hamiltonian perturbation theory assisted by semi-analytical numerical methods. For the accurate evaluation and representation of the resonance driving terms, we constructed a simple numerical tool, the Graphical Representation of Resonances. Using the GRR tool, we were able to identify the deteriorating effect of the large errors in some special quadrupoles with respect to the DA of LHC optics version 5. Further, we identified the (1, –1) resonance which was correlated with the drop of the DA after the introduction of a large skew octupole bias in the dipoles of the LHC optics version 5 "target" error table. In order to recover the lost DA, we used octupole spool pieces which minimised the effect of this resonance. Particle tracking has shown that, by following the proposed correction schemes, the DA of the LHC models under study was considerably improved. We can thus be confident that this type of resonance analysis can be used as a guide in order to achieve an efficient correction of accelerator models. In the near future, the GRR tool will be appropriately standardised and documented in order to be accessible for anyone desiring to perform this type of resonance analysis in a lattice of interest.

REFERENCES

1. Berz, M. et al. *Part. Acc.*, **24**, 91 (1989).
2. Berz, M., *Part. Acc.*, **24**, 109 (1989).
3. Bazzani, A., et al., *CERN Yellow Report*, **94-02**, 1994.
4. Forest, E., "The DaLie Code" (unpublished), 1986.
5. Irwin, J., et al., 4th EPAC Conference, London, 1994.
6. Todesco, E., et al., *Comp. Phys. Commun.* **106**, 169 (1997).
7. Laskar, J. *Physica D*, **67**, 257 (1993).
8. Bartolini, R. and Schmidt, F., *Part.Acc.* **59**, 93 (1998).
9. Schmidt, F., *CERN SL report* **94–56**, 1994.
10. Böge, M., et al., EPAC'96, Barcelona, 1996.
11. Böge , M. and Schmidt, F., PAC'97, Vancouver, 1997.
12. Papaphilippou, Y. and Schmidt, F., *LHC project report* **235**, HEACC'98, Dubna, 1998.
13. Papaphilippou, Y. and Schmidt, F., *LHC project report*, in press (1998).
14. The LHC Study Group, *The Large Hadron Collider*, CERN/AC/95-05(LHC), 1995.
15. Böge , M., Schmidt, F. and Xu, G., *LHC project note* **154**, (1998).
16. Jin, L., Papaphilippou, Y. and Schmidt, F., *LHC project report* **253**, (1998).